Turk J Chem
31 (2007) , 211 – 221.
© TÜBİTAK

Hydrothermal Synthesis, Characterization and Photocatalytic Activity of Nanosized TiO_2 Based Catalysts for Rhodamine B Degradation

Funda SAYILKAN[1], Meltem ASİLTÜRK[2], Şadiye ŞENER[2]*, Sema ERDEMOĞLU[2], Murat ERDEMOĞLU[3] and Hikmet SAYILKAN[1]

[1] *İnönü University, Faculty of Education, Department of Science, 44289, Malatya-TURKEY*

[2] *İnönü University, Faculty of Arts and Science, Department of Chemistry, 44289, Malatya-TURKEY*
e-mail: snsener@inonu.edu.tr

[3] *İnönü University, Faculty of Engineering, Department of Mining Engineering, 44289, Malatya-TURKEY*

Received 07.04.2006

Nanosize crystalline TiO_2 and SiO_2/TiO_2 mixed oxide particles as a photocatalyst for rhodamine B dye (RB) degradation in aqueous media were synthesized by a hydrothermal process at 200 °C. They were characterized using XRD, SEM, FT-IR, UV/VIS and BET analysis. The effects of silica content on the crystallinity and photocatalytic activity of TiO_2 were investigated. Photocatalytic activity of the nano-TiO_2 was compared with that of SiO_2/TiO_2 mixed oxides at the same conditions for degradation of RB, and mixed oxide catalysts showed more effective catalytic activity than the TiO_2. The results revealed that photodegradation of RB proceeds by pseudo-first-order reaction kinetics where the rate constant, k, for degradation of 30 mg/L RB using the catalyst with 0.05 SiO_2/TiO_2 mole ratio is 0.133 min^{-1}.

Key Words: SiO_2/TiO_2 mixed oxides, hydrothermal process, photocatalyst, rhodamine B, photodegradation.

Introduction

The photocatalysis reaction is attracting a great deal of attention from the view points of fundamental science and applications. Recently, this type of reaction has been applied to environmental cleaning by utilizing photocatalytic oxidation of organic compounds by semiconductor materials such as TiO_2, ZnO, CdS, and Fe_2O_3.[1] Among the various semiconductor materials, TiO_2 is the most widely used photocatalyst due to its non-toxicity, high activity, large stability, and low cost.[2] The range of organic pollutants that can be completely photomineralized using TiO_2 is very wide and includes many aromatics, dyes, and pesticides.[3–9] The photocatalytic activity of titania varies depending on its crystallinity, particle size, crystal phase, surface area, and the method of preparation. It is known that anatase form with small particle size and high

*Corresponding author

crystallinity is required to obtain highly active titania photocatalysts.[10] Different preparation methods such as hydrothermal,[11,12] sol-gel,[13−16] and micro emulsion[17] to synthesize nanoparticles of titania have been reported. Hydrothermal synthesis is a promising method to obtain nanocrystalline titania particles. The hydrothermal process, in which the chemical reaction could take place under auto-generated pressure upon heating, is efficient to achieve the crystalline phase at relatively low temperatures. The hydrothermal process proceeds with aqueous and/or non-aqueous systems as the reaction medium and is environmentally friendly since the reactions are carried out in a closed system. The phase, particle size, and crystallinity can easily be controlled by hydrothermal conditions.[18] In particular, the particles prepared through hydrothermal synthesis are expected to have large surface area, smaller crystallite size, and higher stability than those obtained by other methods. Recently, anatase nanoparticles were successfully prepared by this process.[19,20] The anatase phase is essential in photocatalysis applications.[21,22] Further, there have been studies reported concerning the photocatalytic activity of titania-based mixed oxides such as ZrO_2/TiO_2 and SiO_2/TiO_2. Silica-titania mixed oxides have attracted much attention.[23−28] Many researchers reported that silica-titania nanocomposites have higher photoactivity than pure TiO_2.[29,30] When titania is mixed with a suitable amount of silica, the increase in photocatalytic efficiency has been attributed to improved thermal stability, the surface area and surface acidity. The increase in surface area with a reduction in particle size means an increase in the number of active sites on which the electron acceptor and donor are adsorbed and participate in the redox reaction. Additionally, it is reasonable that mixing TiO_2 with SiO_2 is an effective method to improve the content of surface adsorbed water and hydroxyl groups, and hence the photocatalytic activity, because the phase transformation from anatase to rutile is inhibited due to the enhanced thermal stability of titania-silica mixed oxide.[31,32]

To obtain a photocatalyst with high performance, many structural parameters are important, such as crystallite size, crystalline quality, and specific surface area. Thus, in this study, a hydrothermal process was chosen to synthesize both TiO_2 and SiO_2/TiO_2 mixed oxides. The effects of silica content on the crystallinity and photoactivity of TiO_2 were studied. Photocatalytic activity of the catalysts was evaluated using the decolorization of a commercial dye, rhodamine B (RB), under UV light irradiation. The photocatalytic activities of the prepared nanosized SiO_2/TiO_2 mixed oxides were compared to that of pure TiO_2, which was used as a reference catalyst prepared under the same conditions.

Experimental

Materials

Titanium tetraisopropoxide (TTIP), (Alpha; 97%) and tetraethylorthosilicate (TEOS), (Aldrich; 98%) were used as precursors of titania and silica, respectively. n-Propyl alcohol purchased from Riedel de Haen was used as solvent after drying over molecular sieves (Fluka, 3 Å XL8) for a day. The water used in the experiments was doubly distilled and deionized. RB was purchased from a local textile factory in Malatya and used without further purification.

Preparation of nanosized TiO_2, SiO_2/TiO_2 particles and nanosols

The synthesis of nanosized particles was carried out as follows. First TTIP was dissolved in n-propanol. After stirring for 5 min at ambient temperature, an n-propanol-hydrochloride acid mixture was added dropwise

into alkoxide solution at a rate of 1 mL/min. After stirring for 5 min, a water-n-propanol mixture was added to the latter solution dropwise at approximately the same rate. The mixture was stirred at ambient temperature for 10 min. The sol-solution obtained thus was then transferred into a stainless Teflon-lined autoclave and heated at 200 °C for 2 h. The mol ratios of $PrOH^n$/TTIP, H_2O/ TTIP and HCl/ TTIP were 15, 2.62, and 0.2, respectively. The SiO_2/TiO_2 particles were synthesized by adding a mixture of n-propanol-TEOS (prepared with varying amounts of TEOS) into TTIP/n-propanol mixture before HCl/alcohol and water/alcohol mixtures were added at the same drop rate. The mol ratios of H_2O/TTIP, HCl/TTIP, and TEOS/TTIP were 2.7, 0.2, and X (X: 0.0103, 0.0515, and 0.103), respectively. The mixture was stirred at ambient temperature for 10 min. The sol-solutions were then transferred into a stainless Teflon-lined autoclave. The amount of TTIP was 14.11% by weight in all mixtures. The powders obtained by the hydrothermal process were isolated by centrifugation and dried in a vacuum sterilizer at 30 °C for 4 h. Thus, nanosized TiO_2 and 3 kinds of SiO_2/TiO_2 were obtained. Before the examination of the photocatalytic degradation of the dye, TiO_2 and SiO_2/TiO_2 sols were prepared. For this purpose, certain amounts of TiO_2 and SiO_2/TiO_2 were ultrasonically dispersed without addition of any dispersing agent except for X: 0.103 mol ratio of SiO_2/TiO_2. For the preparation of the last oxide mixture sol, SiO_2/TiO_2 (X: 0.103 mol ratio), 4 drops of concentrated HCl solution were added to SiO_2/TiO_2-water mixture prior to dispersing in an ultrasonic bath. In this way, transparent sols were obtained.

The 4 photocatalysts shall be referred to as TiO_2 (without SiO_2), 0.01 SiO_2/TiO_2 (0.0103 SiO_2/TiO_2 mol ratio), 0.05 SiO_2/TiO_2 (0.0515 SiO_2/TiO_2 mol ratio), and 0.1 SiO_2/TiO_2 (0.103 SiO_2/TiO_2 mol ratio).

Characterization

The major phase of the samples was determined from X-ray diffraction patterns obtained using a Rigaku Geigerflex Model D/Max-B diffractometer. Diffraction patterns were taken over the 2θ range 0-70° Average crystallite size of samples was calculated by means of Scherrer's equation. The BET surface areas of samples were determined by nitrogen adsorption data at 77 K using a Micromeritics ASAP 2400 model BET analyzer where the samples were degassed at 130 °C for 4 h before N_2 adsorption. Pore size distribution of the samples was computed by the DFT plus method. Infrared spectra were recorded on a Perkin-Elmer Model 283 model Fourier Transformed Infrared (FT-IR) spectrophotometer, using KBr pellets. The elemental composition and morphology of samples were determined by energy dispersive X-ray analysis (EDX) and scanning electron microscopy (SEM) using a LEO EVO 40 model microscope connected to a Röntek X-flash detector. Zeta (ζ) potential measurements were performed without addition of electrolyte to characterize the surface charge of nanoparticles using a Zeta-Meter System 3.0+ Model zetameter. UV-irradiation was carried out by a Solar Box 1500 model radiation unit with Xe-lamp and a controller to vary the irradiation time and power input from 390 to 1100 W/m^2. The concentration of RB in all aqueous solutions was analyzed using a Shimadzu Model 1601 UV-VIS spectrophotometer.

Photocatalytic degradation experiments

Photodegradation of RB in aqueous media was tested using the synthesized catalysts. To the nanosols of the catalysts was added 750 μL of RB stock solution (1000 μ/L) so as to make up 25 mL of 30 mg/L of dye solutions, in each case. Prior to the irradiation, the reaction mixture was kept in the dark for 15 min to ensure sufficient adsorption of the dye. The mixture was then irradiated with UV light of 770 W/m^2

in the solar box. The samples were collected at regular intervals of time (5, 10, 20, 30, 40, and 50 min) and concentration changes of dye solution were measured using a UV-vis spectrometer at 553 nm (λ_{max}) corresponding to the maximal absorption of the dye.

Photocatalytic degradation kinetics

A Langmuir-Hinshelwood kinetic model is widely used to describe the kinetics of photodegradation of many organic compounds,[7] and is described as

$$r = -dC/dt = kKC/1 + KC \quad (1)$$

where r is the rate of reaction (mol/L.min), C is the equilibrium concentration of reagent (mol/ L), t is the time (min), k is the rate constant (1/min), and K is the Langmuir constant (L/mol). This equation is simplified to a pseudo-first-order expression, when the concentration of reagent being reacted is too low, as

$$r = -dC/dt = kC \quad (2)$$

Equation (2) can be integrated, resulting in

$$lnC_0/C = kt \quad (3)$$

where C is the dye concentration at instant t (mg/L), C_o is the dye concentration at t = 0 (mg/L), k is the pseudo-first-order rate constant (1/min), and t is the irradiation time (min).

Results and Discussion

Characterization of the photocatalysts

Shown in Figure 1 are the powder XRD patterns of the hydrothermally synthesized silica-titania mixed oxides and pure titania nanoparticles. It was observed that all of the XRD patterns of the particles are quite similar. The peaks corresponding to the anatase TiO_2 phase appeared at 2θ = 25.2, 37.8, 48.0, 54.5 and 62.6°. There are sharp and strong peaks of anatase phase 2θ = 25.2° in the XRD patterns of all samples. As shown in Figure 1, all of the titania in these systems were anatase form and the rutile or brookite phase is not observed.

The crystallite size of prepared samples was determined from the line broadening of the peak at 2θ = 25.2° by Scherrer's equation. Some characteristics of the samples, such as crystallite size, BET surface area, micropore area, micropore volume, average pore diameter, and element content, are listed in Table 1. As the SiO_2 to TiO_2 ratio increased, crystallite size increased from 8 to 9.33 nm, but it surprisingly decreased when the ratio was 0.1. The BET surface areas increased with increasing molar ratio of silica to titania from 0.01 to 0.1 and reached a maximum of 134.36 m^2/g. The micropore surface area decreased from 59.08 to 46.04 m^2/g when the Si to Ti ratio was changed from 0.01 to 0.1. The mesopore surface areas were obtained by subtracting micropore surface area from the corresponding BET surface area. The mesopore area for the samples with SiO_2 to TiO_2 ratios of 0.01, 0.05, and 0.1 obtained in this way was 32.2, 68.55, and 88.32 m^2/g, respectively. The ratio of mesopore surface area to total surface area increased from 35.6% to 65.7% when the ratio was varied from 0.01 to 0.1.

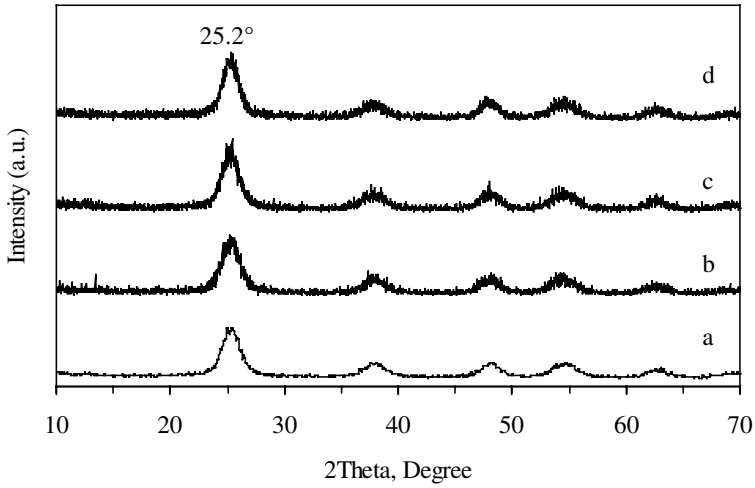

Figure 1. XRD pattern of pure TiO_2 (a), Si/Ti 0.1 (b) Si/Ti 0.05 (c), Si/Ti 0.01 (d).

Table 1. The textural properties of the catalysts.

Sample	Crystallite size of TiO_2 (nm)	S_{BET} (m^2/g)	S_{mi} (m^2/g)	V_{mi} (cm^3/g)	V_{tot} (cm^3/g)	V_{mi}/V_{tot} %	EDX Si% Ti%
TiO_2	8.00	114	43.19	0.023	0.061	37.7	- 99
0.01 SiO_2/TiO_2	9.12	91.30	59.08	0.031	0.046	67.4	0.24 95.72
0.05 SiO_2/TiO_2	9.33	116.32	47.77	0.026	0.072	36.1	3.23 92.66
0.1 SiO_2/TiO_2	8.50	134.36	46.04	0.025	0.060	41.7	3.74 94.19

S_{BET}: BET surface area; S_{mi}: micropore area; V_{mi}: micropore volume; V_{tot}: total volume.

Total pore volumes were estimated from nitrogen adsorption at a relative pressure of 0.98. BET measurements confirmed the absence of macropores in all nanoparticles. The micropore volume decreased up to a ratio of 0.1. The microporosity (percentage of micropore to total pore volume V_{mi}/ V_{tot}) changes between 67.4% and 41.7% for the SiO_2/TiO_2 mixed oxides as shown in Table 1. The mesopore volume was obtained by subtracting micropore volume from the corresponding total volume. The mesoporosity (percentage of mesopore to total pore volume V_{me}/V_{tot}) increased from 3.27% to 64% when the ratio was varied from 0.01 to 0.05. However, there was a decrease in the mesoporosity at a 0.1 SiO_2 to TiO_2 ratio (58%). As a result, microporosity decreased and mesoporosity increased. This increase in the mesoporosity may be the result of the widening of micropores and/or the creation of new pores, possibly affecting the photocatalytic activity of those samples, due to the adsorption of the molecules mainly in the mesopores.

The FT-IR data for the SiO_2/TiO_2 mixed oxides are summarized in Table 2. The FT-IR data in Table 2 are agreement with the results reported by Cheng and coworkers.[33] The peaks observed at 3480 and 1635 cm^{-1} correspond to stretching mode of water and hydroxyl. The peak at 1200 may be due to SiO_2 sides of the crystallites. The weak band at 920 cm^{-1} reveals the interaction between titania and silica at molecular scale.

The SEM microphotographs of samples are shown in Figure 2. The shapes of the particles are quite similar to each other and likely become spherical in general. In the SEM images it is seen that both the pure TiO_2 and SiO_2/TiO_2 particles are agglomerates. The agglomeration may result from the hydrothermal treatment conditions. However, the size distribution of the powder was not determined; the size of the particles varies in the range of 1-8 μm, as measured using the SEM images.

Table 2. The FT-IR data for SiO_2/TiO_2 mixed oxides.

Bands (cm^{-1})	Assignments
920	Si-O-Ti vibration
1060	asymmetric Si-O-Si stretching vibration
800	symmetric Si-O-Si stretching vibration
1635	–OH bending vibration
3480	–OH stretching vibration
1200	SiO_2 sides of the crystallites
2776-2894	C-H stretching of aliphatic $–CH_2$ and $–CH_3$ groups.
630	O-Ti-O vibration
1100	Ti-O-C vibration

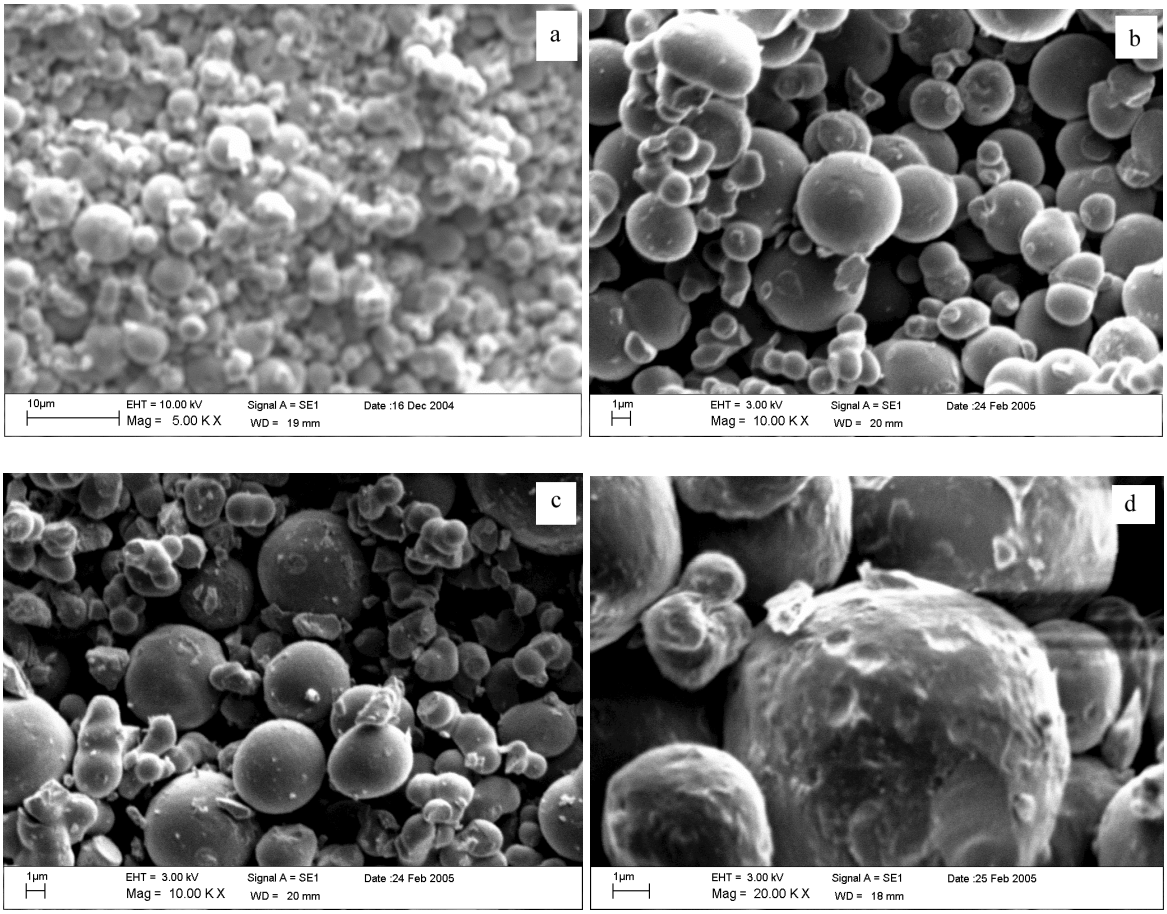

Figure 2. SEM microphotographs of hydrothermally synthesized pure titania (a) and mixed oxides in which SiO_2/TiO_2 is 0.01 (b); 0.05 (c) and 0.1 (d).

Zeta (ζ) potential measurements were performed in order to characterize the surface charge of nanoparticles. The ζ potentials of the nanoparticles in distilled water as a function of the sol pH are given in Figure 3. As seen, the nanoparticles in aqueous solutions are positively charged at the pH range investigated (2.5-4.3). ζ potential measurements could not be carried out for pH $>$ 4.5 due to precipitation in the nanosols. The ζ potentials of SiO_2/TiO_2 nanoparticles increase with a decrease in pH values below 3.4, reach a maximum and then decrease until the pH value of 4.0. The positive charge of the TiO_2 nanoparticle increases with

a decrease in pH, as a result of the increasing degree of protonation of the TiO_2 surface. For example, the charge of TiO_2 is +43.37 mV at pH 3 and +32.72 mV at pH 4.25. For hydrous oxides, the charge determining ions are H^+ and OH^-. These ions establish the charge of the particles by protonating or deprotonating the bonds on the surface of the particles as

$$M - OH + OH^- \rightarrow M - O^- + H_2O$$

$$M - OH + H^+ \rightarrow M - OH_2^+$$

where M is a Si and Ti, and M-OH_2^+, M-OH and M-O^- are positive, neutral and negative surface groups, respectively. For all nanosols and for all pH values applied in this study, charge inversion does not occur. For all nanoparticles, no PZC (point of zero charge) was observed within the pH range applied in this work.

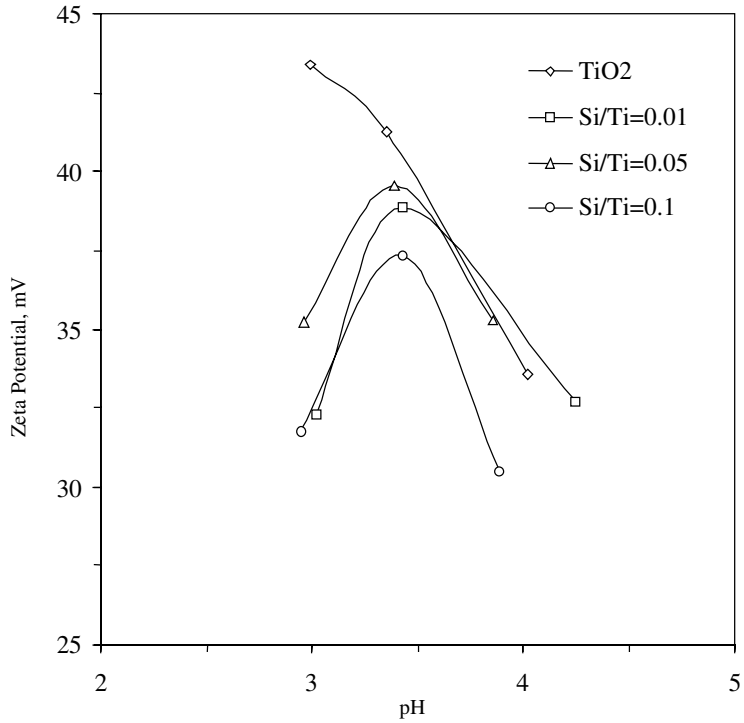

Figure 3. Variation of zeta potential as a function of pH for nanosized SiO_2/TiO_2 mixed oxides and pure TiO_2.

Photodegradation of RB

Degradation of RB under the catalysis of pure TiO_2 and SiO_2/TiO_2 nanoparticles was investigated. Photocatalysis experiments were carried out with 1% (w/w) catalyst sol in water (a proportion determined by a preliminary experiment), dye concentration of 30 mg/L, 60 min reaction time and at natural pH. For the subsequent experiments, the dye solution was kept in the dark for 15 min before irradiating to make sure that adsorption was achieved. In the photolysis experiments no variation in RB concentration was observed.

The experimental data indicated that the silica content of TiO_2 significantly affects photocatalytic activity. The photocatalytic activity of the TiO_2 was compared with that of SiO_2/TiO_2 mixed oxides at the same conditions for degradation of RB and it was found that mixed oxide catalysts showed more effective catalytic activity than the TiO_2. The photocatalytic activity increased as the SiO_2 content was

made 0.05 and then decreased on further increases in the SiO_2 content, which shows that the maximum photocatalytic activity for 0.05 molar ratio of SiO_2 was optimum for photocatalytic activity under the experimental conditions. For instance, Figure 4 illustrates the photocatalytic degradation of RB using 0.05 SiO_2/TiO_2 over time. As seen, the absorbance of RB decreased to almost zero within 50 min. For higher ratios of SiO_2, however, the surface active sites are probably covered by inactive silica. Therefore, 0.1 SiO_2/TiO_2 has the lowest photocatalytic activity, and 0.05 SiO_2/TiO_2 exhibits better photocatalytic activity than the pure TiO_2. Such a difference is ascribed to the smaller crystallite size of TiO_2 (8.0 nm) compared to 0.05 SiO_2/TiO_2 (9.33 nm). A similar observation was reported by Jung et al.,[15] concluding that the photoactivity of titania-based photocatalysts linearly depends on the crystallite size of the anatase phase, and therefore the enlargement of crystallite size is essential for the preparation of a high active photocatalyst.

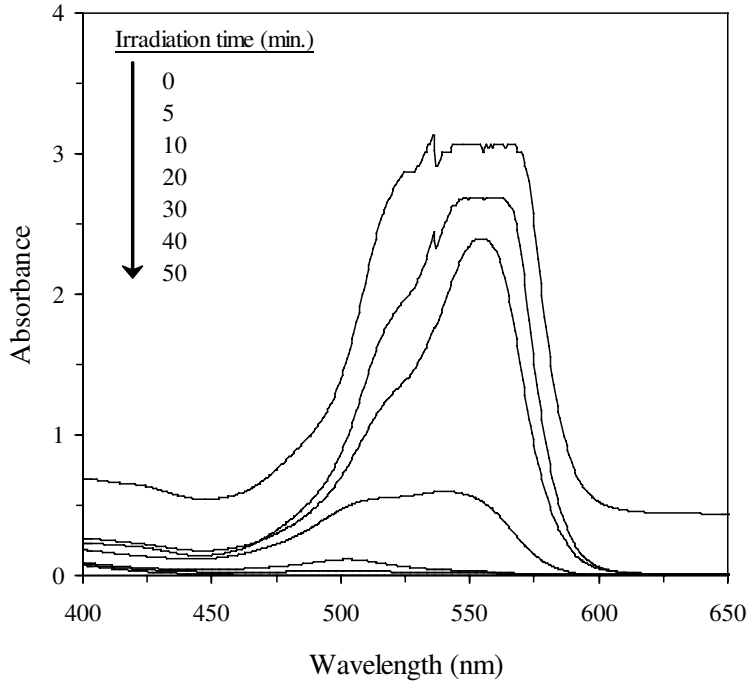

Figure 4. Change in absorbance with time, representing the photodegradation of RB using SiO_2/TiO_2 with a molar ratio of 0.05.

In general, the logarithmic plots of concentration data give a straight line and its slope is pseudo-first-order rate constant. The degradation data were evaluated to facilitate the subsequent mathematical interpretation of all the relevant kinetic parameters, such as the correlation coefficients (R^2) and the degradation rate constants, k. It was found that all reactions were found to follow a pseudo-first-order kinetic, as shown in Figure 5. As seen, the photodegradation rate of RB for 0.05 SiO_2/TiO_2 was faster than that for 0.01 SiO_2/TiO_2 and TiO_2 (without SiO_2). Further increase in SiO_2/TiO_2 from 0.05 to 0.1 molar ratio decreased the photodegradation rate constant from 0.133 to 0.114 min^{-1}.

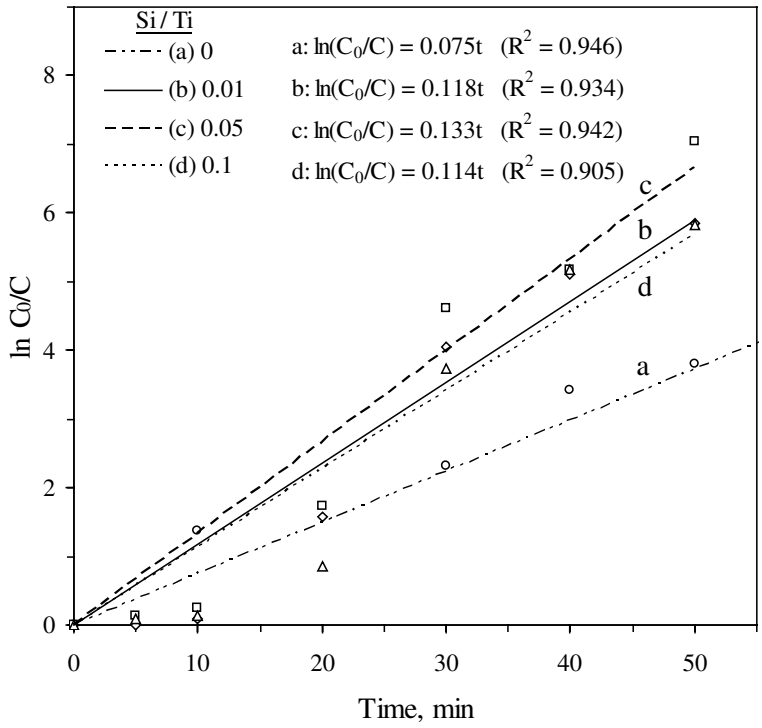

Figure 5. Pseudo-first-order photodegradation kinetics of RB.

It has been reported that the photodegradation of RB results from both de-ethylation and degradation of RB chromophore structure.[34] The changes in the RB concentration with different irradiation times were investigated for nanosols by determining the absorbance at 553 nm. As irradiation time was increased up to 40 min, the intensity of the maximum peak located near 553 nm decreased gradually to near zero. A decreasing λ_{max} at 553 nm reflects the degradation of RB on the nanosols.

De-ethylation of RB is the main reaction occurring at the surface, whereas the RB degradation is predominantly a solution bulk process. According to the study by Zhang et al.,[35] RB is the N,N,N,N'-tetraethylated rhodamine molecule showing λ_{max} at 552 nm. The λ_{max} of RB shifted toward the blue region under UV irradiation (N,N,N'-triethylated rhodamine, at 539 nm; N,N-diethylated rhodamine at 522 nm; N-ethylated rhodamine at 510 nm and rhodamine at 498 nm). Table 3 shows the wavelength shifts of the absorption maximum with different irradiation times on the nanosols.

Table 3. The wavelength shifts of the λ_{max} with different irradiation times.

Catalyst	Wavelength shift at time (min)					
	0	5	10	20	30	40
TiO_2	553	553	553	553	553	498
0.01 SiO_2/TiO_2	553	553	553	538	499	0
0.05 SiO_2/TiO_2	553	553	553	538	500	0
0.1 SiO_2/TiO_2	553	553	553	550	513	498

As seen in Table 3, the complete de-ethylation of pure TiO_2 and 0.1 SiO_2/TiO_2 nanosols occurs after 40 min exposure to irradiation while 0.01 SiO_2/TiO_2 and 0.05 SiO_2/TiO_2 takes 30 min for the same process. The large blue shift in the λ_{max} of RB in the nanosols results from the significant de-ethylation of RB occurring on the nanosols simultaneously with the degradation of the RB.

Conclusions

The following conclusions were drawn from the experimental studies:

- TiO_2-based catalysts were synthesized by hydrothermal method at 200 °C and characterized by various physical techniques. It was found that all of the catalyst have only anatase crystalline phase.

- The BET surface areas increased with increasing molar ratio of silica to titania. The crystallite sizes of samples also increased with increasing silica content.

- The photocatalytic activity of SiO_2/TiO_2 mixed oxides was found to have a linear relationship with the crystallite size of the anatase phase.

- The photodegradation reaction obeyed the rules of a pseudo-first-order kinetic reaction.

- The results showed that 0.05 SiO_2/TiO_2 exhibits better photocatalytic activity than the others, especially than the pure TiO_2.

Acknowledgment

The authors gratefully acknowledge the financial support from İnönü University, Turkey (BAPB-2004/01).

References

1. D.S. Bhatkhande, V.G. Pangarkar and A.A.C.M. Beenackers, **J. Chem. Technol. Biotechnol**. **77,** 102 (2001).
2. C. Hu, Y. Tang, Z. Jiang, Z. Hao, H. Tang and P.K. Wong, **Appl. Catal. A: General 253,** 389 (2003).
3. T. Zhang, T. Oyama, A. Aoshima, H. Hidaka, J. Zhao and N. Serpone, **J. Photochem. Photobiol. A: Chemistry 140,** 163 (2001).
4. Ö. Kartal, M. Erol and H. Oğuz, **Chem. Eng. Technol. 24,** 645 (2001).
5. I. Ilisz, A. Dombi, K. Mogyorosi, A. Farkas and I. Dekany, **Appl. Catal. B: Environmental 39,** 247 (2002).
6. S. Chiron, A. Fernandez-Alba, A. Rodriquez and E. Garcia-Calvo, **Wat. Res. 34,** 366 (2000).
7. Y. Chen, K. Wang and L. Lou, **J. Photochem. Photobiol. A: Chemistry 163,** 281(2004).
8. I. Bouzaida, C. Ferronato, J.M. Chovelon, M.E. Rammah and J.M. Herrmann, **J. Photochem. Photobiol. A: Chemistry 168,** 23 (2004).
9. A. Aguedach, S. Brosillon, J. Morvan and E.K. Lhadi, **Appl. Catal. B: Environmental 57,** 55 (2004).
10. K.Y. Jung and S.B. Park, **Appl. Catal. A: Environmental 25,** 249 (2000).
11. M.M. Yusuf, H. Imai and H. Hirashima, **J. Sol-Gel Sci. Technol., 25,** 65 (2002).
12. Y.V. Kolen'ko, B.R. Churagulov, M. Kunst, L. Mazerolles and C. Colbeau-Justin, **App. Catal. B: Environ., 54,** 51 (2004).
13. Y. Diaoued, S. Badilescu, P.V. Ashirt, D. Bersani, P.P. Lottici and J. Robichaud, **J. Sol- Gel Sci. Technol., 24,** 255 (2002).
14. C. Su, B.Y. Hong and C.M. Tseng, **Catal. Today, 96,** 119 (2004).
15. K.Y. Jung and S.B. Park, **Mater. Lett., 58,** 2897 (2004).

16. H. Bala, J. Zhao, Y. Jiang, X. Ding, Y. Tian, K. Yu and Z. Wang, **Mater. Lett., 59,** 1937 (2005).
17. Y. Bessekhouad, D. Robert and J.W. Veber, **J. Photochem. Photobiol. A: Chemistry, 157,** 47 (2003).
18. Y.V. Kolen'ko, B.R. Churagulov, M. Kunst, L. Mazerolles and C. Colbeau-Justin, **Appl. Catal. A: Environmental 54,** 51 (2004).
19. F. Sayılkan, S. Erdemoğlu, M. Asiltürk, M. Akarsu, Ş. Şener, H. Sayılkan, M. Erdemoğlu and E. Arpaç, **Mat. Res. Bull. 41,** 2276 (2006).
20. M. Asiltürk, F. Sayılkan, S. Erdemoğlu, M. Akarsu, H. Sayılkan, M. Erdemoğlu and E. Arpaç, **J. Hazard. Mater. 129,** 164 (2006).
21. J. Yang, S. Mei and J.M.F. Ferreira, **J. Europ. Ceram. Soc. 24,** 335 (2004).
22. M. Kang, S-J. Choung and J.Y. Park, **Catal. Today 87,** 87 (2003).
23. A.A. Ismail, I.A. Ibrahim, M.S. Ahmed, R.M. Mohamed and H. Ell-Shall, **J. Photochem. Photobiol. A: Chemistry 163,** 445 (2004).
24. M.S. Vohra and K. Tanaka,**Wat. Res. 37,** 3992 (2003).
25. Y. Zhang, G. Xiong, N. Yao, W. Yang and X. Fu, **Catal. Today 68,** 89 (2001).
26. K. Guan, **Surf. Coat. Technol. 191,** 155 (2005).
27. Z. Feng, L. Kaiming, W. Guoliang, S. Hua and H. Anmin, **J. Cryst. Growth 264,** 297 (2004).
28. P. Cheng, M. Zheng, Y. Jin, Q. Huang and M. Gu, **Mater. Lett. 4276,** 1 (2002).
29. J. Yu, J.C. Yu and X. Zhao, **J. Sol-Gel Sci. Tech. 24,** 95 (2002).
30. S. Hong, M.S. Lee, S. Park and G. Lee, **Catal. Today 87,** 99 (2003).
31. C. Xie, Z. Xu, Q. Yang, B. Xue, Y. Du and J. Zhang, **Mater. Sci. Eng. B 112,** 34 (2004).
32. K.Y. Jung, S.B. Park and S. Ihm, **Appl. Catal. B: Environmental 51,** 239 (2004).
33. P. Cheng, M. Zheng, Q. Huang, Y. Jin, and M. Gu, **J. Mater. Sci. Lett. 22,** 1165 (2003).
34. H.M. Sung-Suh, J.R. Choi, H.J. Hah, S.M. Koo and Y.C. Bae, **J. Photochem. Photobiol. A: Chemistry 163,** 37 (2004).
35. Y. Zhang, H. Xu, Y. Xu, H. Zhang and Y. Wang, **J. Photochem. Photobiol. A: Chemistry, 170,** 279 (2005).